Available online at www.sciencedirect.com

SCIENCE DIRECT

Metabolism Clinical and Experimental 55 (2006) 203–212

Metabolism
Clinical and Experimental

www.elsevier.com/locate/metabol

High-fat feeding effects on components of the CAP/Cbl signaling cascade in Sprague-Dawley rat skeletal muscle

Jeffrey R. Bernard, Donald W. Reeder, Henry J. Herr, Donato A. Rivas, Ben B. Yaspelkis III*

Department of Kinesiology, College of Health and Human Development, California State University Northridge, Northridge, CA 91330-8287, USA

Received 5 April 2005; accepted 21 August 2005

Abstract

The aim of this investigation was to determine whether the CAP (Cbl-associated protein)/Cbl signaling cascade is present and responsive to insulin in skeletal muscle and if high-fat feeding impairs insulin-stimulated activation of this signaling cascade. Sprague-Dawley rats were assigned to either control (n = 16) or high fat–fed (n = 16) dietary groups. After a 12-week dietary period, animals were subjected to hind limb perfusions in the presence (n = 8 per group) or absence (n = 8 per group) of insulin. High-fat feeding reduced rates of insulin-stimulated skeletal muscle phosphatidylinositol 3-kinase activity and 3-*O*-methylglucose transport. In plasma membrane fractions, neither the high-fat diet nor insulin altered the insulin receptor β subunit (IR-β), APS (adaptor protein containing PH and SH2 domains), c-Cbl, or TC10 protein concentration, but high-fat feeding did decrease CAP protein concentration. APS, c-Cbl, CAP, and TC10 messenger RNA were present in the skeletal muscle and reflected the protein concentration of experimental groups. Despite insulin-stimulated plasma membrane IR-β tyrosine phosphorylation being unaffected by high-fat feeding, c-Cbl tyrosine phosphorylation, the kinase activity of IR-β toward APS, and glucose transporter 4 protein concentration were all significantly reduced in insulin-stimulated plasma membrane prepared from the skeletal muscle of high fat–fed animals. These findings suggest that the CAP/Cbl signaling cascade is present in skeletal muscle, activated by insulin, and impaired by high-fat feeding.

1. Introduction

Insulin-stimulated activation of insulin receptor substrate-1 (IRS-1)–associated phosphatidylinositol 3-kinase (PI3K) is required for glucose transporter translocation [1-3], and an extensive body of literature exists that implicates defects of the PI3K-dependent or "classic" insulin signaling cascade as the primary defect that contributes to insulin resistance and impaired carbohydrate metabolism in skeletal muscle. However, it appears that in insulin-sensitive tissues, the activation of the PI3K-dependent pathway alone cannot fully account for insulin-stimulated glucose transport and glucose transporter 4 (GLUT4) translocation [4-6]. A body of literature is beginning to emerge that implicates the involvement of a "novel" insulin signaling pathway that is also activated in response to insulin stimulation [7-9].

In response to insulin, the adaptor protein APS (adaptor containing PH and SH2 domains) recruits c-Cbl to the insulin receptor along with a second adaptor protein CAP (Cbl-associated protein) [10-12]. c-Cbl is then phosphorylated on multiple tyrosine residues, followed by the disassociation and translocation of the CAP/c-Cbl complex to the lipid rafts subdomains [10-12], which results in the activation of small guanosine triphosphate–binding proteins that facilitate GLUT4 translocation to the plasma membrane [13-15]. Although the activation of the CAP/Cbl signaling cascade has garnered some preliminary evaluation in skeletal muscle obtained from genetic [16] and pharmacologically induced models [17] of insulin resistance, to the best of our knowledge, the involvement and activation of this pathway have not been evaluated in skeletal muscle obtained from high fat–fed rodents. It appears that this pathway is likely to be involved in insulin-stimulated skeletal muscle glucose transport as components of this pathway are highly expressed in skeletal muscle [10,18,19]. Therefore, it is the intent of this investigation to more fully characterize the CAP/Cbl signaling cascade in normal and high fat–fed

* Corresponding author. Tel.: +1 818 677 7509; fax: +1 818 677 7514.
E-mail address: ben.yaspelkis@csun.edu (B.B. Yaspelkis).

0026-0495/$ – see front matter © 2006 Elsevier Inc. All rights reserved.
doi:10.1016/j.metabol.2005.08.013

rodent skeletal muscle under basal and insulin-stimulated conditions and to determine if this pathway is altered in skeletal muscle obtained from high fat–fed rodents.

2. Materials and methods

2.1. Experimental design

Thirty-two male Sprague-Dawley rats approximately 6 weeks of age, weighing between 185 and 220 g were obtained from Harlan (San Diego, CA). Animals were randomly assigned to either control (CON, n = 16) or high fat–fed (HF, n = 16) dietary groups. The control diet consisted of 20% fat-derived energy (no. 112386, Dyets, Bethlehem, PA), and the high-fat diet consisted of 59% fat-derived energy (no. 112387, Dyets). This high-fat diet has previously been shown to induce skeletal muscle insulin resistance [20-22].

All experimental procedures were approved by the Institutional Animal Care and Use Committee at California State University, Northridge, and conformed to the guidelines for the use of laboratory animals published by the US Department of Health and Human Resources.

2.2. Surgical preparation and hind limb perfusions

After the 12-week dietary period, all animals were subjected to hind limb perfusion as we have described previously [20,21,23,24]. Perfusions were performed in the presence (n = 8 per group) or absence (n = 8 per group) of 500 μU/mL insulin at a flow rate of 7.5 mL/min. The perfusate consisted of 30% washed time-expired human erythrocytes, Krebs Henseleit buffer (KHB), 4% dialyzed bovine serum albumin (Fisher Scientific, Fair Lawn, NJ), and 0.2 mmol/L pyruvate that was continuously gassed with a mixture of 95% O_2-5% CO_2 and warmed to 37°C. The hind limbs were washed out with perfusate containing 1 mmol/L glucose for 5 minutes in preparation for the measurement of glucose transport. Glucose transport was measured over an 8-minute period using an 8 mmol/L concentration of nonmetabolized glucose analogue 3-*O*-methylglucose (3-MG) (32 μCi 3-[^{3}H]MG per mmol/L, PerkinElmer Life Sciences, Boston, MA) and 2 mmol/L mannitol (60 μCi-[1-^{14}C]mannitol per mmol/L, PerkinElmer Life Sciences). Perfusions were limited to 13 minutes (5 minutes washout and 8 minutes transport), as it has previously been shown in 3T3-L1 adipocytes that c-Cbl phosphorylation significantly decreases after 15 minutes of insulin stimulation [12]. Immediately after the transport period, portions of the red and white quadriceps (RQ and WQ, respectively) were excised from both hind limbs, blotted on gauze dampened with cold KHB, freeze-clamped in liquid nitrogen, and stored at −80°C for later analysis.

2.3. 3-O-Methylglucose transport

Rates of insulin-stimulated skeletal muscle 3-MG transport were calculated as previously described [20,22,25].

2.4. Muscle homogenization

Muscle samples were weighed and homogenized 1:10 in homogenization buffer (HB) that contained 50 mmol/L HEPES, 150 mmol/L NaCl, 200 mmol/L sodium pyrophosphate, 20 mmol/L β-glycerolphosphate, 20 mmol/L NaF, 2 mmol/L sodium vanadate, 20 mmol/L EDTA, 1% IGPAL, 10% glycerol, 2 mmol/L phenylmethylsufonyl fluoride, 1 mmol/L $MgCl_2$, 1 mmol/L $CaCl_2$, 10 μg/mL leupeptin, and 10 μg/mL aprotinin. Muscles were homogenized on ice using a glass Pyrex homogenizer and centrifuged at 18 300*g* for 15 minutes at 4°C (Micromax RF, International Equipment, Needham Heights, MA). The supernatant was collected and quantified for protein content by the Bradford [26] method.

2.5. IRS-1–associated PI3K activity

IRS-1–associated PI3K activity was determined as have been described previously [21].

2.6. Plasma membrane fractionation

Plasma membrane fractions were prepared as we [21,25,27] and others [28-30] have described previously. The final plasma membrane pellet was resuspended in 200 μL of HB per gram of original tissue weight, frozen in liquid nitrogen, and stored at −80°C for later analysis. The activity of the plasma membrane marker enzyme 5′-nucleotidase was assessed as previously described [21] in plasma membrane fractions and compared with the activity in crude homogenate fractions to ensure that purified plasma membrane fractions were being used for analysis. Characterization of the membrane fractions obtained is presented in Table 1.

2.7. Plasma membrane insulin receptor β subunit, flotillin, TC10, and GLUT4 protein concentrations

Insulin receptor β subunit (IR-β), flotillin, TC10, and GLUT4 protein concentrations were determined in plasma membrane fractions obtained from the RQ. Sample protein (50 μg for IR-β, flotillin, and GLUT4, and 70 μg for TC10) was subjected to sodium dodecyl sulfate–polyacrylamide gel electrophoresis (SDS-PAGE) run under reducing

Table 1
Membrane fractionation characterization

	Basal		Insulin	
	Normal diet (n = 8)	High-fat diet (n = 8)	Normal diet (n = 8)	High-fat diet (n = 8)
5′-Nucleotidase activity (nmol · min^{-1} · mg protein^{-1})				
Plasma membrane	330.22 ± 57.3	405.72 ± 72.2	314.35 ± 66.7	354.22 ± 68.8
Crude homogenate	57.72 ± 11.0	50.33 ± 9.9	57.00 ± 11.4	48.36 ± 14.0
Fold increase	7.2 ± 2.1	8.2 ± 2.8	8.9 ± 2.6	10.8 ± 2.4
Percentage of yield	13.5 ± 5.2	16.6 ± 7.2	16.2 ± 7.4	22.4 ± 4.8

Values are expressed as means ± SE.

Table 2
Primer sequences

	Sense	Antisense
APS	5′-CTCCTGACAGAAGCAGA-3′	5′-CTGACACCACCTGAAGAC-3′
c-Cbl	5′-AGAATGTTCATCCTCCTATTGC-3′	5′-TCCTCGTGTGGCTGATTATAG-3′
CAP	5′-AAGCCTCGTCCACCTAAG-3′	5′-CTGCCTGCCAAGTCAATC-3′
TC10	5′-TATGCCAACGACGCCTTC-3′	5′-ACGATCATAGTCTTCCTGTCC-3′
β-Actin	5′-GCCTTCCTTCCTGGGTATG-3′	5′-ATCTCCTTCTGCATCCTGTC-3′

conditions on either a 10% (IR-β, flotillin, GLUT4) or a 12.5% (TC10) resolving gel using a MiniProtean 3 dual slab cell (BioRad) and transferred to a polyvinylidene difluoride (PVDF) membrane using a semidry transfer unit. The membranes were blocked in 5% nonfat dry milk (NFDM)/Tris-Tween–buffered saline and incubated with affinity-purified rabbit polyclonal anti–IR-β subunit (cat. no. 06-492, Upstate USA [UBT], Charlottesville, VA), mouse monoclonal anti–flotillin-1 (cat. no. 610820, BD Transduction Laboratories, BD Biosciences Pharmingen, San Diego, CA), goat polyclonal anti-TC10 (sc-12637, Santa Cruz Biotechnology [SCBT], Santa Cruz, CA), or rabbit polyclonal anti-GLUT4 (donated by Dr Samuel W. Cushman, National Institute of Diabetes and Digestive and Kidney Diseases, Bethesda, MD) followed by the species-specific immunoglobulin (Ig) G secondary antibody conjugated to horseradish peroxidase (HRP). Antibody binding was visualized by enhanced chemiluminescence in accordance to the manufacturer's instructions (West Femto, Pierce Chemical, Rockford, IL). Images were captured by using a charge-coupled device camera in a ChemiDoc system (BioRad, Hercules, CA) and saved to a Macintosh G4 computer. Density of the bands was quantified with Quantity One analysis software (BioRad) and expressed as a percentage of a standard run on each gel.

2.8. Plasma membrane APS, c-Cbl, and CAP protein concentrations

APS, c-Cbl, and CAP protein concentrations were determined in plasma membrane fractions obtained from the RQ. Sample protein (400 μg for APS, 300 μg for c-Cbl, 200 μg for CAP) was incubated with anti-APS (sc-8894, SCBT), anti–c-Cbl (cat. no. 05-440, UBT), or anti-CAP (cat. no. 06-994, UBT) overnight at 4°C. After the overnight incubation, 100 μL of protein A–sepharose (PRO-A) slurry (Amersham Pharmacia Biotechnology, Piscataway, NJ) was added to the immunoprecipitates and rotated for 1.5 hours at 4°C. The immunocomplexes were then washed as previously described [21]. After the last wash, 20 μL of a 1:1 solution of 2× treatment buffer and HB was added to each sample, boiled for 5 minutes at 100°C, and centrifuged for 20 seconds in a minicentrifuge. Ten microliters of supernatant were subjected to SDS-PAGE run under reducing conditions on either a 7.5% (c-Cbl, CAP) or a 10% (APS) resolving gel. The resolved proteins were transferred to a PVDF membrane and blocked in 5% NFDM/TTBS. The membranes were then incubated with affinity-purified anti-APS (sc-8894, SCBT), anti–c-Cbl, (cat no. 05-440, UBT), or anti-CAP (cat. no. 06-994, UBT), followed by incubation with the species-specific IgG secondary antibody conjugated to HRP. Antibody binding was visualized and quantified as described above.

2.9. Plasma membrane IR-β and c-Cbl tyrosine phosphorylation

Insulin receptor β subunit and c-Cbl tyrosine phosphorylation was determined in plasma membrane fractions obtained from the RQ. Sample protein (500 μg for IR-β, 300 μg for c-Cbl) was incubated with 4 μg of either anti–IR-β subunit (cat. no. 06-492, UBT) or anti–c-Cbl (cat. no. 05-440, UBT) overnight at 4°C. After the overnight incubation, 100 μL of PRO-A slurry was added to the immunoprecipitates and treated as described above. Ten microliters of supernatant was subjected to SDS-PAGE run under reducing conditions on either a 7.5% (c-Cbl) or a 10% (IR-β) resolving gel. The resolved proteins were transferred to a PVDF membrane and blocked in 5% NFDM/TTBS. The membranes were then incubated with affinity-purified polyclonal antiphosphotyrosine (cat. no. 06-427, UBT), followed by incubation with goat antirabbit IgG (sc-2004, SCBT) conjugated to HRP. Antibody binding was visualized and quantified as described above.

2.10. APS, c-Cbl, CAP, and TC10 mRNA

Total RNA was isolated from portions of the RQ from the non–insulin-stimulated (basal) animals using the RNA Wiz reagent isolation kit (Ambion, Austin, TX). Total isolated RNA was quantified using UV spectrophotometry at 260 and 280 nm. Only samples with an Abs_{260}-to-Abs_{280} ratio of 1.7:2.2 were used for further analysis. After quantification, RNA integrity was determined by electrophoresis and UV visualization.

Table 3
Rates of 3-MG transport

Muscles	Basal		Insulin	
	Control (n = 8)	High fat–fed (n = 8)	Control (n = 8)	High fat–fed (n = 8)
RQ	3.92 ± 0.17	3.40 ± 0.24	7.04 ± 0.40*,**,***	5.07 ± 0.28*,**
WQ	1.95 ± 0.34	1.97 ± 0.29	2.35 ± 0.34	2.26 ± 0.32

Values are expressed as means ± SE (μmol · h^{-1} · g^{-1}).
* $P < .05$, significantly different from CON BAS.
** $P < .05$, significantly different from HF BAS.
*** $P < .05$, significantly different from HF INS.

Contaminating DNA was removed from samples using a DNA-free kit (Ambion). Samples were then requantified as described above to determine the concentration of total purified RNA. Two micrograms of total purified RNA was reverse transcribed using a Retroscript kit (Ambion) with oligo dT primers (Ambion) according to the manufacturer's instructions. The reverse transcription (RT) products were stored at −20°C until further analysis by quantitative polymerase chain reaction (qPCR).

2.11. *Rattus norvegicus*

APS, c-Cbl, CAP, TC10, and β-actin gene sequences were obtained from GenBank and imported to Beacon Designer primer design software version 3.0 (Lab Velocity, San Francisco, CA). Primers for APS, c-Cbl, CAP, TC10, and β-actin (Table 2) were synthesized by Integrated DNA Technologies (Carlsbad, CA). β-Actin messenger RNA (mRNA) served as the housekeeping gene for quantification purposes. Two microliters of RT product were used in a real-time PCR reaction with the 1-μmol/L primers listed above and IQ Supermix (BioRad) at a final volume of 30 μL. Annealing temperatures were optimized for each primer pair to ensure the absence of secondary product formation.

Two microliters of the RT product was used in a PCR reaction using the iQ Superscript SYBR Green Mix

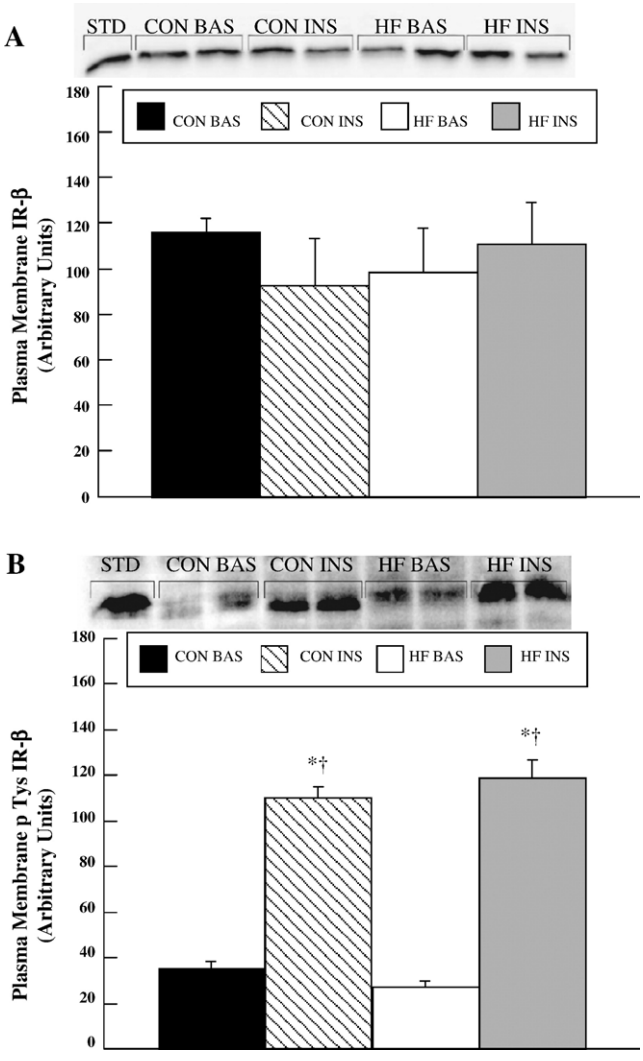

Fig. 1. Plasma membrane IR-β subunit protein concentration (A) and tyrosine-phosphorylated IR-β subunit (B) obtained from the RQ of CON BAS (n = 8), CON INS (n = 8), HF BAS (n = 8), or HF INS (n = 8) animals. Values are expressed as means ± SE. * $P < .05$, significantly different from CON BAS; † $P < .05$, significantly different from HF BAS. STD indicates standard.

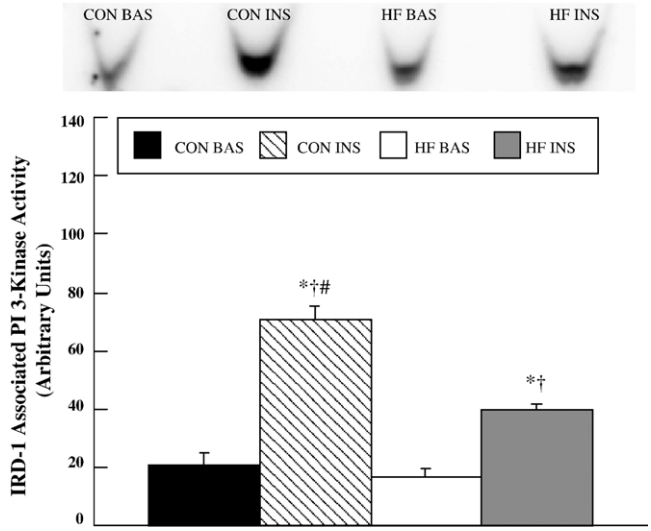

Fig. 2. IRS-1–associated PI3K activity obtained from the RQ of CON BAS (n = 8), CON INS (n = 8), HF BAS (n = 8), or HF INS (n = 8) animals. Values are expressed as means ± SE. * $P < .05$, significantly different from CON BAS; † $P < .05$, significantly different from HF BAS; # $P < .05$, significantly different from HF INS.

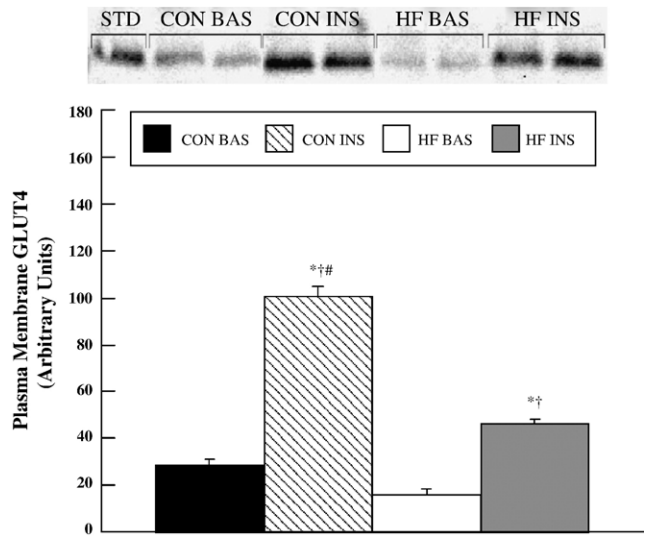

Fig. 3. Plasma membrane GLUT4 protein concentration obtained from the RQ of CON BAS (n = 8), CON INS (n = 8), HF BAS (n = 8), or HF INS (HF INS, n = 8) animals. Values are expressed as means ± SE. * $P < .05$, significantly different from CON BAS; † $P < .05$, significantly different from HF BAS; # $P < .05$, significantly different from HF INS.

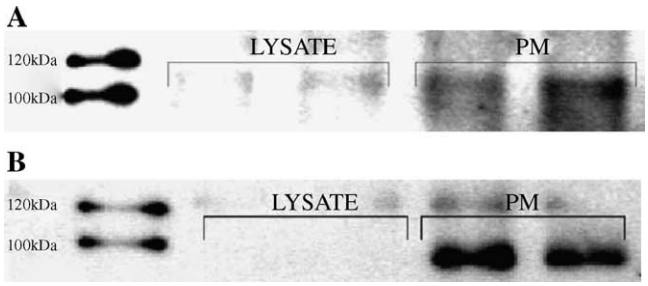

Fig. 4. Lysate and plasma membrane c-Cbl (A) and CAP protein concentrations (B) obtained from the RQ of control insulin (CON INS) animals.

(BioRad) according to the manufacturer's instructions in an iCycler (BioRad) equipped with an optical module (BioRad). Final primer concentration for each primer pair was 250 nmol/L. With the optimized annealing temperatures for each primer pair, qPCR was carried out using SYBR Green–based quantification. A standard curve was created for each PCR product amplified using a serial dilution (1:3) of the complementary DNA sample used for optimization. Polymerase chain reaction efficiency for each amplification was determined from the serial dilution by comparing the differences in critical threshold (C_T) values for each standard. Reactions with at least 85% efficiency were considered suitable for reliable data acquisition. C_T values for APS, c-Cbl, CAP, and β-actin were imported into the *q-gene macro* to determine the relative gene expression, as described by Muller et al [31].

2.12. IR-β kinase activity toward APS

The IR-β kinase activity toward APS was determined in insulin-stimulated plasma membrane fractions obtained from the RQ. IR-β kinase activity toward APS was not detectable under basal conditions. Two hundred fifty micrograms of sample protein was incubated with 4 μg of anti–IR-β subunit (cat. no. 06-492, UBT) overnight at 4°C. After the overnight incubation, 100 μL of PRO-A slurry was added to the immunoprecipitates and placed on rotation for 1.5 hours at 4°C. The immunocomplexes were then washed once in buffers A and B and twice in buffer C, as previously described [21]. After the final wash, the supernatant was completely removed. Twenty microliters of assay dilution buffer (UBT) was added to the immunocomplex in addition to 10 μL of an APS substrate. The APS substrate, amino acid sequence 610 to 621 (ARAVENQYSFY) of the APS SH2 domain containing a single tyrosine that is phosphorylated in response to insulin stimulation, was synthesized by Invitrogen (Carlsbad). The kinase reaction was initiated by the addition of assay dilution buffer (UBT), 75 mmol/L $MgCl_2$, 1 mol/L adenosine triphosphate, and [γ-^{32}P] adenosine triphosphate (PerkinElmer Life Sciences), and warmed to 37°C with constant mixing for 10 minutes. The reaction was terminated by the addition of Tris-tricine sample buffer and heating at 95°C for 5 minutes. Fifteen microliters were loaded onto a 20% Tris-tricine polyacrylamide gel in duplicate and electrophoresed for 150 minutes at 110 V using a MiniProtean electrophoresis system (BioRad). After electrophoreses, gels were wrapped in plastic wrap and

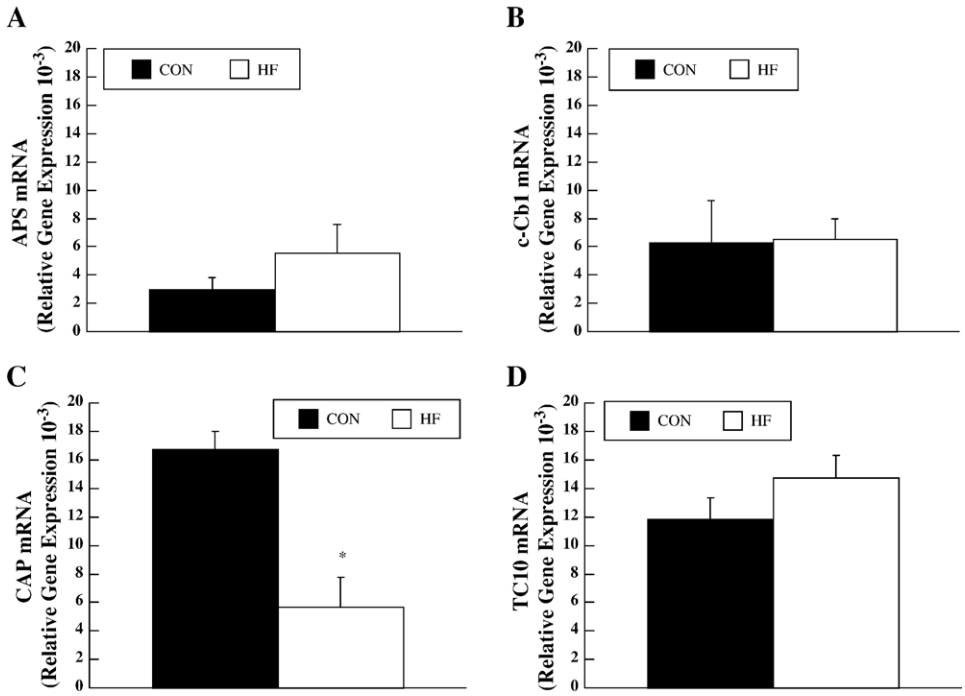

Fig. 5. APS (A), c-Cbl (B), CAP (C), and TC10 (D) mRNA expression obtained from the RQ of CON (n = 8), or HF (n = 8) basal animals. Values are expressed as means ± SE. * $P < .05$, significantly different from CON.

exposed to a phosphor screen (BioRad) overnight. Images were captured and quantified as described above.

2.13. Statistical analysis

A 1-way analysis of variance was used on all variables to determine whether significant differences exist between groups. When a significant F ratio was obtained, a Tukey HSD post hoc test was used to identify statistically significant differences ($P < .05$) among the means. Statistical analyses were performed using JMP software (SAS Institute, Cary, NC), and all values were expressed as means ± SE.

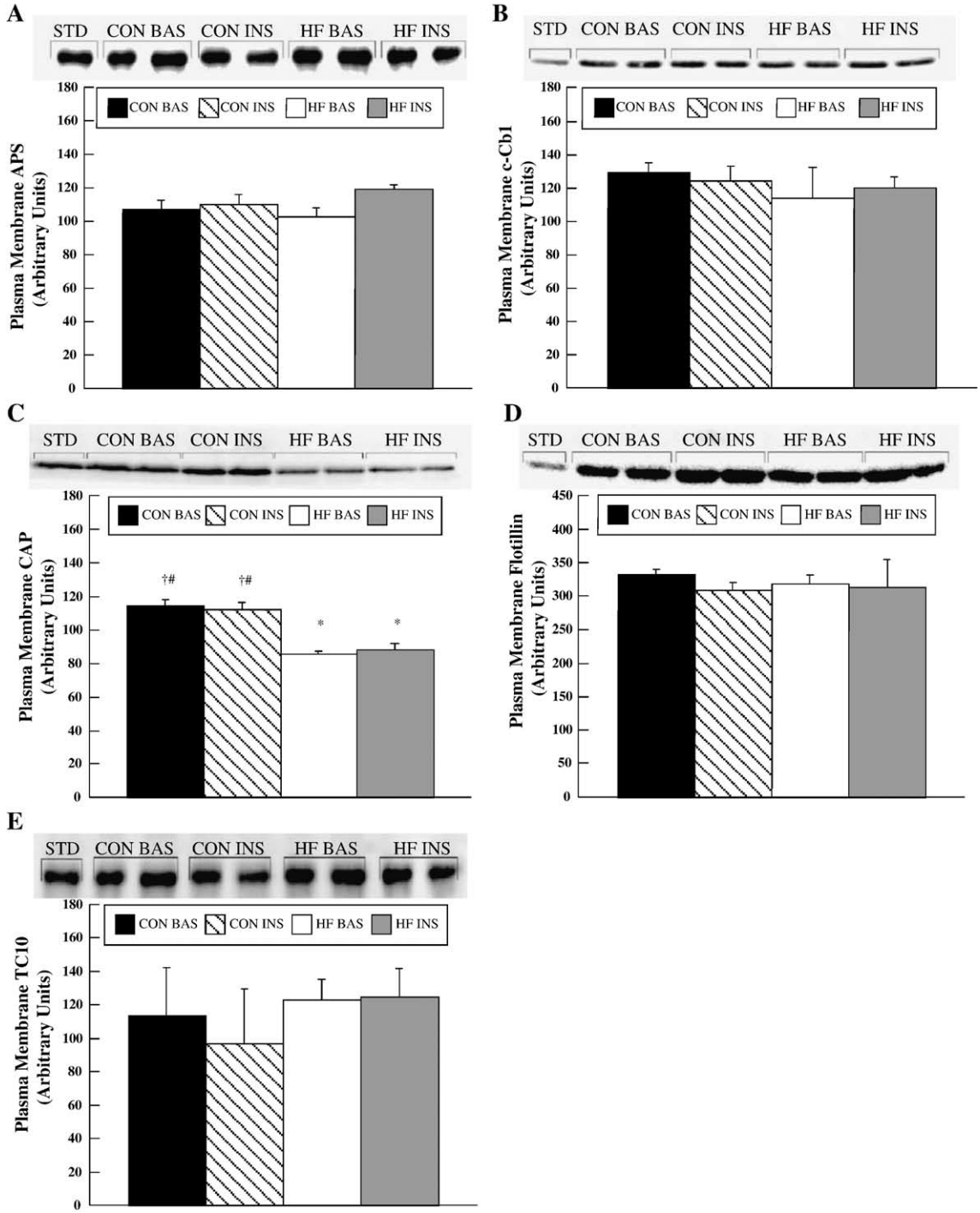

Fig. 6. Plasma membrane APS (A), c-Cbl (B), CAP (C), flotillin (D), and TC10 (E) protein concentrations obtained from the RQ of CON BAS (n = 8), CON INS (n = 8), HF BAS (n = 8), or HF INS (n = 8) animals. Values are expressed as means ± SE. * $P < .05$, significantly different from CON BAS; † $P < .05$, significantly different from HF BAS; # $P < .05$, significantly different from HF INS.

3. Results

3.1. Body and epididymal fat pad mass

At the onset of the dietary period, the body mass of control basal (CON BAS; 202.1 ± 6.1 g), control insulin (CON INS; 198.1 ± 3.0 g), high fat–fed basal (HF BAS; 204.2 ± 3.3 g), and high fat–fed insulin (HF INS; 203.0 ± 3.5 g) animals were similar. Although the body mass of all animals increased throughout the study, no significant differences in body mass were observed among CON BAS (472.8 ± 10.3 g), CON INS (477.3 ± 12.3 g), HF BAS (488.1 ± 11.3 g), and HF INS (491.7 ± 11.9 g) animals at the end of the 12-week dietary period. At the end of the dietary period, the epididymal fat pad mass of the HF BAS (11.6 ± 1.0 g) and HF INS (12.3 ± 1.1 g) animals exhibited a trend (P = .09) to be heavier than the CON BAS (10.0 ± 1.2 g) and CON INS (9.0 ± 0.5 g) animals.

3.2. Glucose transport

Rates of 3-MG transport were similar across fiber types and experimental groups in the absence of insulin (Table 3). In the presence of insulin, 3-MG transport was increased above basal levels in the RQ of the control and high fat–fed animals. However, rates of 3-MG transport in the RQ of the high fat–fed animals were less than that of the control-diet animals. The high-fat diet had no effect on rates of insulin-stimulated 3-MG transport in the WQ. As the high-fat diet did not affect rates of 3-MG transport in the WQ, we restricted all additional measurements to the RQ.

3.3. Insulin signaling

Plasma membrane IR-β subunit protein concentration (Fig. 1A) and tyrosine phosphorylation (Fig. 1B) were unchanged by high-fat feeding, and insulin significantly increased IR-β subunit phosphorylation in both the CON INS and HF INS animals compared with basal groups. However, insulin receptor phosphorylation stimulated by insulin was not affected by high-fat feeding.

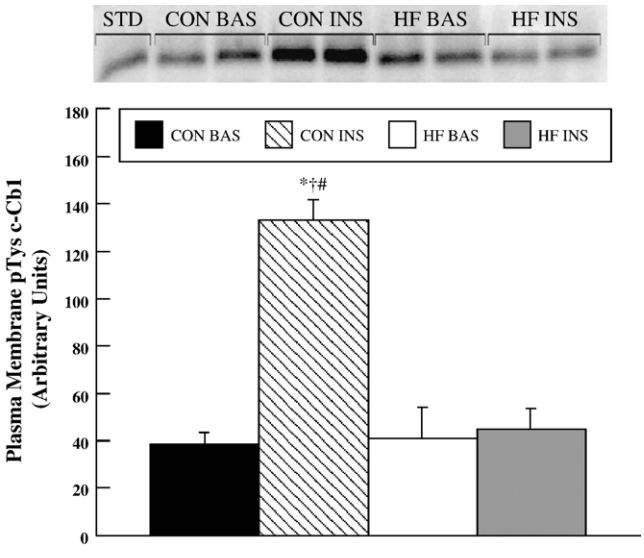

Fig. 7. Plasma membrane tyrosine-phosphorylated c-Cbl obtained from the RQ of CON BAS (n = 8), CON INS (n = 8), HF BAS (n = 8), or HF INS (HF INS, n = 8) animals. Values are expressed as means ± SE. * P < .05, significantly different from CON BAS; † P < .05, significantly different from HF BAS; # P < .05, significantly different from HF INS.

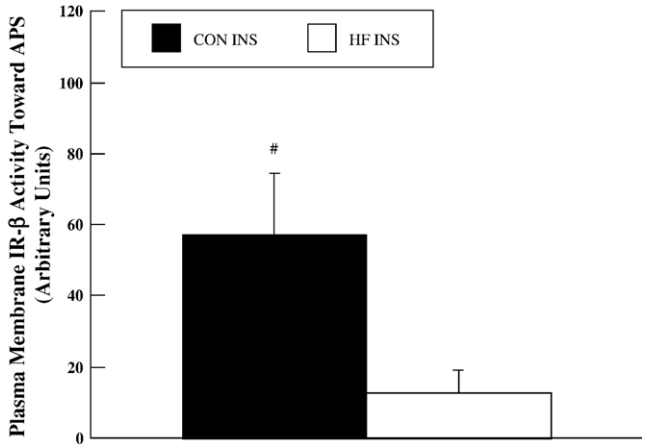

Fig. 8. Plasma membrane IR-β kinase activity toward APS obtained from the RQ of CON INS (n = 8) or HF INS (HF INS, n = 8) animals. Values are expressed as means ± SE. # P < .05, significantly different from HF INS.

We have previously shown that impaired IRS-1–associated PI3K activity is a defect of the classic insulin signaling cascade in high-fat diet–induced insulin-resistant rodent skeletal muscle [20-22]. To provide confirmation that the high-fat diet did affect components of the classic pathway and glucose transporter translocation, we assessed insulin-stimulated skeletal muscle IRS-1–associated PI3K activity and plasma membrane GLUT4 protein concentration. In the absence of insulin, IRS-1–associated PI3K activity was not different in the skeletal muscle assessed (Fig. 2). Although insulin increased PI3K activity above basal levels in both the CON INS and HF INS animals, rates of activity were greater in the skeletal muscle of the CON INS animals compared with HF INS animals. Similarly, insulin increased the plasma membrane GLUT4 protein concentration, but the high-fat diet resulted in a reduced number of glucose transporters becoming associated with the plasma membrane (Fig. 3).

Although c-Cbl (Fig. 4A) and CAP (Fig. 4B) were not detectable in muscle lysates, APS (Fig. 5A), c-Cbl (Fig. 5B), CAP (Fig. 5C), and TC10 (Fig. 5D) mRNA were quantifiable. The high-fat diet did not alter APS, c-Cbl, flotillin, or TC10 mRNA, but did decrease CAP mRNA. Plasma membrane protein concentration mirrored the mRNA. Specifically, the high-fat diet did not affect APS (Fig. 6A), c-Cbl (Fig. 6B), flotillin (Fig. 6D), or TC10 (Fig. 6E), but did decrease CAP (Fig. 6C) protein concentration. Insulin did not alter the plasma membrane–associated APS, c-Cbl, CAP, flotillin, or TC10 protein concentration in either the CON or the HF animals when compared with the absence of insulin.

The high-fat diet also affected the activation of the CAP/Cbl signaling cascade. c-Cbl tyrosine phosphorylation (Fig. 7) was decreased in the plasma membrane of the HF INS animals compared with CON INS animals. Similarly, the insulin-stimulated IR-β kinase activity toward an APS substrate (Fig. 8) was significantly decreased in plasma membrane fractions of the HF INS animals compared with CON INS animals.

4. Discussion

Providing confirmation that the high-fat diet induced skeletal muscle insulin resistance, we show that 3-MG transport was reduced in the RQ of the high fat–fed animals and is in excellent agreement with a number of previous investigations that have also shown a high-fat diet to decrease insulin-stimulated glucose uptake and 3-MG transport in rodent skeletal muscle [20,21,25,32-37]. Reduced rates of insulin-stimulated 3-MG transport in skeletal muscle of high fat–fed rodents have been attributed to reduced total GLUT4 protein concentration and/or the impaired ability to effectively translocate GLUT4 to the plasma membrane [22,25,33,38]. Consistent with these previous reports is our observation that insulin-stimulated plasma membrane GLUT4 protein concentration was reduced in the high fat–fed animals. Furthermore, it has been reported that PI3K activity is decreased in the skeletal muscle of high fat–fed rodents and is associated with decreased rates of insulin-stimulated 3-MG transport [20-22,38,39], which is supported by our finding that PI3K activity was significantly reduced in response to high-fat feeding. However, there has been controversy regarding the effect of high-fat feeding on the insulin receptor. It has been previously shown that 8 weeks of high-fat feeding may [40] or may not [33] impair IR-β phosphorylation. In the present investigation, we observed no difference in plasma membrane IR-β protein concentration or IR-β tyrosine phosphorylation between the CON INS and HF INS animals. Collectively, these observations support the contention that the high-fat diet induced insulin resistance, in part, by impairing components of the classic insulin signaling cascade and glucose transporter translocation.

As the CAP/Cbl signaling cascade has not been extensively evaluated in skeletal muscle, we first investigated components of this pathway in normal rodent skeletal muscle. It should be noted though that there is some controversy as to whether the CAP/Cbl signaling pathway even exists in skeletal muscle. Although it has been reported that L6 myoblasts express very little CAP [41], others [18,41] have reported CAP to be readily detectable in L6 myotubes. In addition, CAP may [16] or may not [17] exist in rodent skeletal muscle. We report here that APS, CAP, flotillin, and TC10 proteins exist in skeletal muscle, and it appears that each protein is primarily associated with the plasma membrane as the presence or absence of insulin had no effect on their plasma membrane concentration. These findings are in agreement with previous reports using adipocytes, indicating that APS [11], CAP [11], flotillin [12], and TC10 [42] are constitutively localized to the plasma membrane under basal and insulin-stimulated conditions. In contrast, c-Cbl associates with the plasma membrane of 3T3-L1 adipocytes in response to insulin, but appears to be localized to the low-density microsomal fraction under basal conditions [12,13].

We next assessed whether a high-fat diet altered components of the CAP/Cbl signaling cascade in skeletal muscle and found that neither basal and insulin-stimulated plasma membrane protein concentration nor mRNA of APS, c-Cbl, flotillin, or TC10 protein was altered by high-fat feeding. However, the high-fat diet did decrease both plasma membrane CAP protein concentration and CAP mRNA. Although we observed no difference in plasma membrane c-Cbl protein concentration in the presence or absence of insulin, it is possible that c-Cbl localization may not be altered in skeletal muscle. It should also be highlighted that Thirone et al [17] were unable to detect CAP in skeletal muscle lysates. In agreement with this group, we too were unable to detect quantifiable amounts of either c-Cbl or CAP in muscle lysates from either basal or insulin-stimulated animals in the experimental groups. However, when plasma membrane fractions were used, as opposed to lysates, the components of this pathway were detectable. In addition, we found that the mRNA for components of the CAP/Cbl signaling cascade did exist in skeletal muscle and paralleled our findings with respect to the plasma membrane concentration of these proteins. Of interest, Molero et al [43] reported that whole-body insulin action and skeletal muscle glucose uptake were improved in c-Cbl–deficient mice. Why these differences exist among investigations is not readily apparent but may be related to the c-Cbl knockout mice having reduced adipose mass and increased circulating levels of leptin, which we have shown can contribute to increased rates of insulin-stimulated glucose transport in skeletal muscle [21,25].

It has been questioned whether insulin activates the CAP/Cbl signaling cascade in skeletal muscle [16-18,43]. Alcazar et al [18] recently reported that insulin caused tyrosine-phosphorylated c-Cbl in L6 myotubes, but in skeletal muscle lysates, insulin caused moderate, but not statistically significant, c-Cbl tyrosine phosphorylation. Thirone et al [17] also reported that insulin did not stimulate c-Cbl tyrosine phosphorylation in muscle lysate. In contrast, when we assessed insulin-stimulated c-Cbl tyrosine phosphorylation in plasma membrane fractions prepared from CON INS animals, we observed enhanced tyrosine-phosphorylated c-Cbl compared with CON BAS animals. Moreover, in high fat–fed skeletal muscle, insulin-stimulated tyrosine phosphorylation of c-Cbl was significantly reduced compared with the CON INS animals. In addition, we have also recently found that insulin-stimulated skeletal muscle c-Cbl tyrosine phosphorylation is enhanced in response to long-term aerobic exercise [23]. However, it has been observed in

adipocytes that the CAP/Cbl pathway may not be required for insulin-stimulated GLUT4 translocation [44,45]. Nevertheless, our findings do indicate that insulin does stimulate tyrosine phosphorylation of c-Cbl and high-fat feeding impairs insulin-stimulated c-Cbl tyrosine phosphorylation in skeletal muscle, but the functional significance of this observation remains to be elucidated.

In an attempt to provide an explanation for this observation, we assessed the kinase activity of IR-β toward APS, an adaptor protein that facilitates c-Cbl recruitment to the insulin receptor. Despite no difference existing between the CON INS and HF INS animals in plasma membrane IR-β protein concentration and IR-β tyrosine phosphorylation, the substrate specific activity of IR-β toward APS was impaired in high fat–fed skeletal muscle. Of interest, it has been reported that a CAP mutant blocks insulin-stimulated tyrosine phosphorylation of Cbl in 3T3-L1 adipocytes by possibly mistargeting c-Cbl or APS [46]. Although we observed that the high-fat diet decreased CAP concentration, the functional significance of this observation was not readily apparent. However, it is plausible to suggest that the decreased CAP concentration may have also contributed to decreasing c-Cbl tyrosine phosphorylation in the high fat–fed skeletal muscle.

In summary, high-fat feeding reduced insulin-stimulated skeletal muscle PI3K activity and rates of 3-MG transport. In plasma membrane fractions prepared from perfused skeletal muscle, it was found that neither the high-fat diet nor insulin altered IR-β, APS, c-Cbl, flotillin, or TC10 protein concentrations. However, plasma membrane CAP protein concentration was reduced in the skeletal muscle from high fat–fed animals, but was unaffected by insulin stimulation. In addition, APS, c-Cbl, CAP, and TC10 mRNA were present in the skeletal muscles and reflected the protein concentration of experimental groups. Despite insulin-stimulated IR-β tyrosine phosphorylation being unaffected by high-fat feeding, plasma membrane c-Cbl tyrosine phosphorylation, the kinase activity of IR-β toward APS, and GLUT4 protein concentration were significantly reduced in the skeletal muscle of high fat–fed animals. Collectively, these findings suggest that in skeletal muscle the CAP/Cbl signaling cascade is present, activated by insulin, and that components of the CAP/Cbl signaling cascade are impaired by high-fat feeding.

Acknowledgment

This investigation was supported in part by the National Institutes of Health grants GM-48680, GM-08395, and DK-57625.

References

[1] Cheatham B, Vlahos CJ, Cheatham L, et al. Phosphatidylinositol 3-kinase activation is required for insulin stimulation of pp70 S6 kinase, DNA synthesis, and glucose transporter translocation. Mol Cell Biol 1994;14:4902-11.

[2] Kanai F, Ito K, Todaka M, et al. Insulin-stimulated GLUT4 translocation is relevant to the phosphorylation of IRS-1 and the activity of PI3-kinase. Biochem Biophys Res Commun 1994;195:762-8.

[3] Yeh J-I, Gulve EA, Rameh L, et al. The effects of wortmannin on rat skeletal muscle. J Biol Chem 1995;270:2107-11.

[4] Guilherme A, Czech MP. Stimulation of IRS-1–associated phosphatidylinositol 3-kinase and Akt/Protein Kinase B but not glucose transport by b1-integrin signaling in rat adipocytes. J Biol Chem 1998;273:33119-22.

[5] Isakoff SJ, Taha C, Rose E, et al. The inability of phosphatidylinositol 3-kinase activation to stimulate GLUT4 translocation indicates additional signaling pathways are required for insulin-stimulated glucose uptake. Proc Natl Acad Sci U S A 1995;92:10247-51.

[6] Staubs PA, Nelson JG, Reichart DR, et al. Platelet-derived growth factor inhibits insulin stimulation of insulin receptor substrate-1–associated phosphatidylinositol 3-kinase in 3T3-L1 adipocytes without affecting glucose transport. J Biol Chem 1998;273:25139-47.

[7] Khan AH, Pessin JE. Insulin regulation of glucose uptake: a complex interplay of intracellular signalling pathways. Diabetologia 2002;45:1475-83.

[8] Saltiel AR, Pessin JE. Insulin signaling pathways in time and space. Trends Cell Biol 2002;12:65-71.

[9] Watson RT, Pessin JE. Intracellular organization of insulin signaling and GLUT4 translocation. Recent Prog Horm Res 2001;56:175-93.

[10] Ribon V, Printen JA, Hoffman NG, et al. A novel, multifunctional c-Cbl binding protein in insulin receptor signaling in 3T3-L1 adipocytes. Mol Cell Biol 1998;18:872-9.

[11] Liu J, Kimura A, Baumann CA, et al. APS facilitates c-Cbl tyrosine phosphorylation and GLUT4 translocation in response to insulin in 3T3-L1 adipocytes. Mol Cell Biol 2002;22:3599-609.

[12] Liu J, DeYoung SM, Hwang JB, et al. The roles of Cbl-b and c-Cbl in insulin-stimulated glucose transport. J Biol Chem 2003;278:36754-62.

[13] Baumann CA, Ribon V, Kanzaki M, et al. CAP defines a second signalling pathway required for insulin-stimulated glucose transport. Nature 2000;407:202-7.

[14] Chiang SH, Baumann CA, Kanzaki M, et al. Insulin-stimulated GLUT4 translocation requires the CAP-dependent activation of TC10. Nature 2001;410:944-8.

[15] Chang L, Adams RD, Saltiel AR. The TC10-interacting protein CIP4/2 is required for insulin-stimulated Glut4 translocation in 3T3L1 adipocytes. Proc Natl Acad Sci U S A 2002;99:12835-40.

[16] Wadley GD, Bruce CR, Konstantopoulos N, et al. The effect of insulin and exercise on c-Cbl protein abundance and phosphorylation in insulin-resistant skeletal muscle in lean and obese Zucker rats. Diabetologia 2004;47:412-9.

[17] Thirone AC, Carvalheira JB, Hirata AE, et al. Regulation of Cbl-associated protein/Cbl pathway in muscle and adipose tissues of two animal models of insulin resistance. Endocrinology 2004;145:281-93.

[18] Alcazar O, Ho RC, Fujii N, et al. cDNA cloning and functional characterization of a novel splice variant of c-Cbl–associated protein from mouse skeletal muscle. Biochem Biophys Res Commun 2004;317:285-93.

[19] Neudauer CL, Joberty G, Tasis N, et al. Distinct cellular effects and interactions of the Rho-family GTPase TC10. Curr Biol 1998;8:1151-60.

[20] Krisan AD, Collins DE, Crain AM, et al. Resistance training enhances components of the insulin signaling cascade in normal and high-fat–fed skeletal muscle. J Appl Physiol 2004;96:1691-700.

[21] Singh MK, Krisan AD, Crain AM, et al. High-fat diet and leptin treatment alter skeletal muscle insulin-stimulated phosphatidylinositol 3-kinase activity and glucose transport. Metabolism 2003;52:1196-205.

[22] Yaspelkis III BB, Singh MK, Krisan AD, et al. Chronic leptin treatment enhances insulin-stimulated glucose disposal in skeletal muscle of high-fat fed rodents. Life Sci 2004;74:1801-16.

[23] Bernard JR, Crain AM, Rivas DA, et al. Chronic aerobic exercise enhances classical and novel insulin signaling in Sprague Dawley rat skeletal muscle. Acta Physiol Scand 2005;183:357-66.

[24] Yaspelkis III BB, Ansari L, Ramey EA, et al. Chronic leptin administration increases insulin-stimulated skeletal muscle glucose uptake and transport. Metabolism 1999;48:671-6.

[25] Yaspelkis III BB, Davis JR, Saberi M, et al. Leptin administration improves skeletal muscle insulin responsiveness in diet-induced insulin-resistant rats. Am J Physiol Endocrinol Metab 2001;280: E130-42.

[26] Bradford MM. A rapid and sensitive method for the quantitation of microgram quantities of protein utilizing the principle of protein-dye binding. Anal Biochem 1976;72:248-54.

[27] Yaspelkis III BB, Saberi M, Singh MK, et al. Chronic leptin treatment normalizes basal glucose transport in a fiber type-specific manner in high-fat–fed rats. Metabolism 2002;51:859-63.

[28] Turcotte LP, Swenberger JR, Tucker MZ, et al. Training-induced elevation in $FABP_{pm}$ is associated with increased palmitate use in contracting muscle. J Appl Physiol 1999;87:285-93.

[29] Ahmed A, Taylor PM, Rennie MJ. Characteristic of glutamate transport in sarcolemmal vesicles from rat skeletal muscle. Am J Physiol Endocrinol Metab 1990;259:E284-91.

[30] Turcotte LP, Srivastava AK, Chiasson J-L. Fasting increases plasma membrane fatty acid–binding protein (FAMPPM) in red skeletal muscle. Mol Cell Biochem 1997;166:153-8.

[31] Muller P, Janovjak H, Miserez A, et al. Processing of gene expression data generated by quantitative real-time RT-PCR. Biotechniques 2002; 32:1372-9.

[32] Wilkes JJ, Bonen A, Bell RC. A modified high-fat diet induces insulin resistance in rat skeletal muscle but not adipocytes. Am J Physiol Endocrinol Metab 1998;275:E679-86.

[33] Hansen PA, Han DH, Marshall BA, et al. A high fat diet impairs stimulation of glucose transport in muscle. Functional evaluation of potential mechanisms. J Biol Chem 1998;273:26157-63.

[34] Buettner R, Newgard CB, Rhodes CJ, et al. Correction of diet-induced hyperglycemia, hyperinsulinemia, and skeletal muscle insulin resistance by moderate hyperleptinemia. Am J Physiol Endocrinol Metab 2000;278:E563-9.

[35] Halseth AE, Bracy DP, Wasserman DH. Limitation to basal and insulin-stimulated skeletal muscle glucose uptake in the high-fat–fed rat. Am J Physiol Endocrinol Metab 2000;279:E1064-71.

[36] Barnard RJ, Roberts CK, Varon SM, et al. Diet-induced insulin resistance precedes other aspects of the metabolic syndrome. J Appl Physiol 1998;84:1311-5.

[37] Kraegen EW, James DE, Storlein LH, et al. In vivo insulin resistance in individual peripheral tissues of the high fat fed rat: assessment by euglycaemic clamp plus deoxyglucose administration. Diabetologia 1986;29:192-8.

[38] Tremblay F, Lavigne C, Jacques H, et al. Defective insulin-induced GLUT4 translocation in skeletal muscle of high fat–fed rats is associated with alterations in both Akt/protein kinase B and atypical protein kinase C (ζ/λ) activities. Diabetes 2001;50:1901-10.

[39] Zierath JR, Houseknecht KL, Gnudi L, et al. High-fat feeding impairs insulin-stimulated GLUT4 recruitment via an early insulin-signaling defect. Diabetes 1997;46:215-23.

[40] Youngren JF, Paik J, Barnard RJ. Impaired insulin-receptor autophosphorylation is an early defect in fat-fed, insulin-resistant rats. J Appl Physiol 2001;91:2240-7.

[41] JeBailey L, Rudich A, Huang X, et al. Skeletal muscle cells and adipocytes differ in their reliance on TC10 and Rac for insulin-induced actin remodeling. Mol Endocrinol 2004;18:359-72.

[42] Watson RT, Pessin JE. Subcellular compartmentalization and trafficking of the insulin-responsive glucose transporter, GLUT4. Exp Cell Res 2001;271:75-83.

[43] Molero JC, Jensen TE, Withers PC, et al. c-Cbl–deficient mice have reduced adiposity, higher energy expenditure, and improved peripheral insulin action. J Clin Invest 2004;114:1326-33.

[44] Zhou QL, Park JG, Jiang ZY, et al. Analysis of insulin signaling by RNAi-based gene silencing. Biochem Soc Trans 2004;32: 817-21.

[45] Mitra P, Zheng X, Czech MP. RNAi-based analysis of CAP, Cbl, and CrkII function in the regulation of GLUT4 by insulin. J Biol Chem 2004;279:37431-5.

[46] Kimura A, Baumann CA, Chiang SH, et al. The sorbin homology domain: a motif for the targeting of proteins to lipid rafts. Proc Natl Acad Sci U S A 2001;98:9098-103.